Journal of Ceramic Processing Research. Vol. 19, No. 4, pp. 290~295 (2018)

JOURNAL OF
Ceramic
Processing Research

Characterization of broadband dielectric properties of aerosol-deposited Al_2O_3 thick films

Oh-Yun Kwon[a,*], Dong-won Lee[b], Jong-Min Oh[c], Jangbom Chai[d] and Byung-Sung Kim[a]
[a]*College of Information and Communication Engineering, Sungkyunkwan University, Suwon 16419, South Korea*
[b]*Material Technology Center, Korea Testing Laboratory, Seoul 152-718, South Korea*
[c]*Department of Electronic Materials Engineering, Kwangwoon University, Seoul 01897, South Korea*
[d]*Department of Mechanical Engineering, Ajou University, Suwon 443-749, South Korea*

The dielectric properties of aerosol-deposited Al_2O_3 thick films were successfully investigated in broadband frequency ranges. Al_2O_3 thick films have been prepared through aerosol deposition on Cu substrate at room temperature. In order to measure the dielectric constants (ε_r) and dielectric losses (tanδ) at microwave frequency, a circular-patch capacitor (CPC) was formed on the Al_2O_3 films through the photo-lithography process. In order to evaluate the parasitic effect of the CPC structure based on measurement results, 3-D electromagnetic simulations were performed. After correction of the measured data including the parasitic components of the CPC, it was observed that the ε_r of the Al_2O_3 thick films slightly decreased with the increase in frequency from 9.7 at 1 GHz, different from the low-frequency results. The corrected tanδ of the Al_2O_3 thick films was 0.03 at 1 GHz and less than 0.05 up to 5 GHz.

Key words: Aerosol-deposition, Microwave dielectric properties, Al_2O_3 thick films, Characterization of dielectric properties.

Introduction

Wireless systems for mobile communication have recently continued to develop in order to satisfy customer demands in terms of multi-functionality and large data transfer. There have been an increasing number of attempts to adapt radio frequency (RF) and microwave systems (such as the upcoming fifth generation mobile communication system) into the current wireless system [1, 2].

The complexity and number of components in such systems have increased as the number of frequency bands has evolved. The system integration technologies of today have evolved from 2-dimensional integration to 3-dimentional integration, such as in system-on-package (SOP) [3] and system-in-package (SIP) [4] schemes. In order to properly realize these schemes, a crucial issue is the material selection for the substrate. Ceramic substrates are a good candidate for SOP and SIP schemes due to their high reliability and good dielectric properties at RF and microwave frequency. Nevertheless, ceramics have some fundamentally weak characteristics as integrated substrates in that they require high processing-temperatures over 1000 °C. For this reason, low temperature process for ceramics has been developed, such as low temperature co-fired ceramics [5]. However, the processing temperature is still too high for integration with silicon-based active devices and for the attachment of metallic transmission lines [6].

The aerosol deposition (AD) process is one of the promising candidates for next-generation fabrication technology for integrated RF and microwave systems due to its various advantages such as room-temperature processing, high deposition rate, and so on [7, 8]. Through the AD process, dielectric thick films with several tens of μm thickness can be rapidly formed on various substrates such as, ceramic, metal, and glass [9, 10]. Moreover, the deposition of metals and polymers has been successfully performed, as well as that of ceramics [11-15].

Although previous studies have been successful in the fabrication of dielectric thick films through the AD process for high-frequency applications, the dielectric properties of the thick film have mainly been measured in the kHz-MHz frequency range due to difficulties in measurement [11, 16, 17]. Furthermore, previous studies on the fabrication of RF and microwave devices such as band pass filters (BPFs) through the AD process has also been successfully carried out, but the characterization of the dielectric properties of the devices' substrates has not been measured at the frequency range of several GHz [18-20]. In this study, the Al_2O_3 thick films were fabricated on a copper (Cu) substrate through the AD process, and the characterization of the dielectric properties of the thick films was performed

*Corresponding author:
Tel : +031-290-7225
Fax: +031-299-4643
E-mail: kwonoy@skku.edu

for the first time in the kHz-GHz frequency range for RF and microwave applications.

Experimental

The dielectric thick films were fabricated through the AD process. The AD process is based on the shock-loading solidification of ultrafine ceramic particles through impact with a substrate after the particles are accelerated using a carrier gas and a nozzle. The particles are then mixed by means of a carrier gas and a vibration system in the aerosol chamber where they are aerosolized. The aerosolized particles are accelerated through a nozzle by the pressure difference between the aerosol chamber and the deposition chamber. Then, thick and dense films are formed by impacting these accelerated particles onto the substrate as depicted in Fig. 1.

The deposition parameters used for the AD process are summarized in Table 1. The details of the AD process apparatus have been previously reported elsewhere [19, 20]. Al_2O_3 powder with a purity of 99.3% (Showa-Denko K.K., A-161SG) was used as the starting powder. The microstructures and crystallinity of the Al_2O_3 films were examined through field-emission scanning electron microscopy (FE-SEM, S-4700, HITACHI Ltd., Japan) and X-ray diffrectometer (XRD, X'Pert PRO, PNAalytical), respectively. The thicknesses of the coating layers were measured using a surface profilometer. The dielectric properties were measured from 10 kHz to 1 MHz using an impedance analyzer (HP4194A). For the low-frequency measurement, gold (Au) electrodes with a 1.0-mm diameter were coated on by sputtering. For the high-frequency measurement, copper (Cu) electrodes were formed on the Al_3O_3 thick film through photo-lithography. The resistivity of the Cu layer deposited by electron-beam evaporation was 2.97 $\mu\Omega\cdot$cm. In the photo-lithography processing, spin-coating, pre-baking, exposure, reversal baking, flood exposure, and development were applied to the aerosol-deposited Al_2O_3 thick films. Photoresist (AZ 5214 E) was used for the mask in the course of the pattering. Electromagnetic modeling and simulation of 3-D full-wave electro-magnetic (EM) fields was performed using HFSS (ANSYS), which solves Maxwell's equations through a numerical analysis based on a finite element method. The complex reflection coefficients of a device under test (DUT) were measured using a vector network analyzer (Agilent) and a probe station with GSG probes (Cascade). A one-port short-open-load calibration was performed using standard substrates (Cascade).

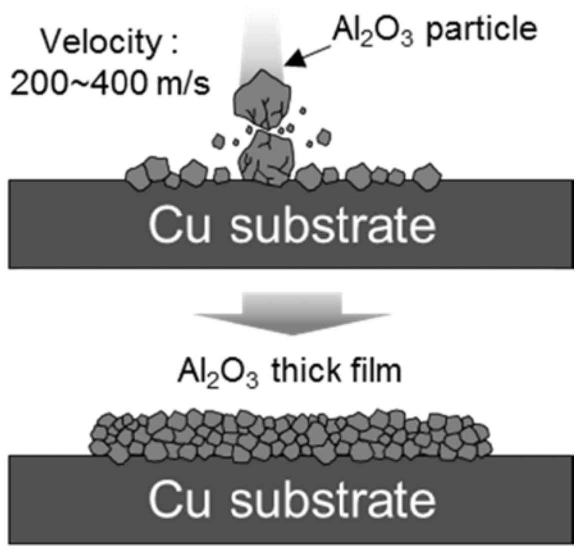

Fig. 1. Schematic diagram of the fabrication of ceramic thick films through the AD process.

Table 1. Deposition conditions of thick films fabricated through the AD process.

Consumption of carrier gas	1-10 L/min
Scanning speed of the nozzle motion	1 mm/sec
Working pressure	5-20 Torr
Size of nozzle orifice	10 mm × 0.4 mm
Distance between substrate and nozzle	5-15 mm
Deposition temperature	Room temperature
Deposition time	10-30 min
Deposition area	10 mm × 20 mm

Results and Discussion

It has been revealed in prior studies that the consolidation and densification phenomena for the AD process are strongly influenced by the size and mechanical properties of the starting powder [17]. The diameters of the craters in aerosol-deposited films can be increased by the mechanical impact of aerosolized Al_2O_3 particles above 1-µm. In order to form a flat Al_2O_3 film, the generation of craters as well as their expansion should be reduced throughout the growth of Al_2O_3 films, and the generation and expansion of these craters is closely associated with the size of the starting Al_2O_3 powder. Therefore, Al_2O_3 starting powder with 0.5-µm size was prepared in this study as shown in Fig. 2(a).

The frequency dependence and losses of the aerosol-deposited films at low-frequency range can be minimized through a heat treatment and a ball milling process of the starting powder [16]. The Al_2O_3 starting powder was heated at 900°C for 2 hrs in an electric furnace in the atmosphere in order to remove any residual moisture and impurities before deposition in this study. A post-annealing process of the Al_2O_3 films in an electric furnace under N_2 atmosphere was additionally performed at 280°C for 5 hrs to enhance the dielectric properties. Fig. 2(b) shows a plane-view SEM image of Al_2O_3 thick films aerosol deposited by

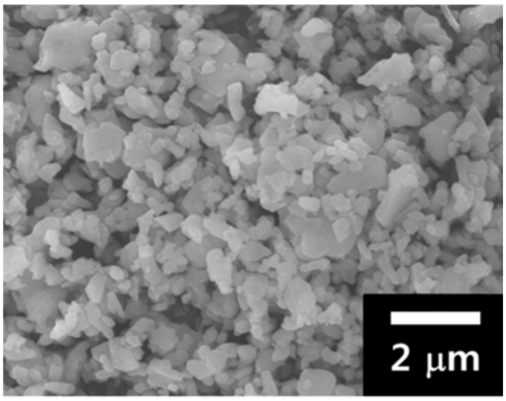

(a)

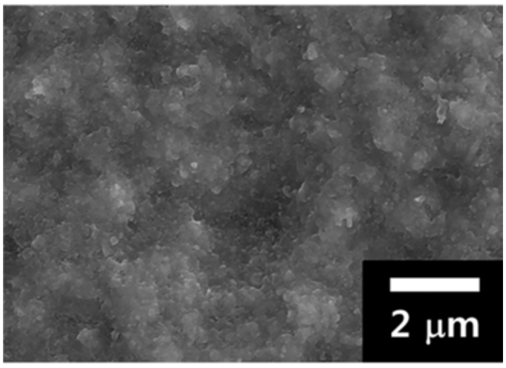

(b)

Fig. 2. SEM images of (a) Al_2O_3 powders and (b) Al_2O_3 thick films.

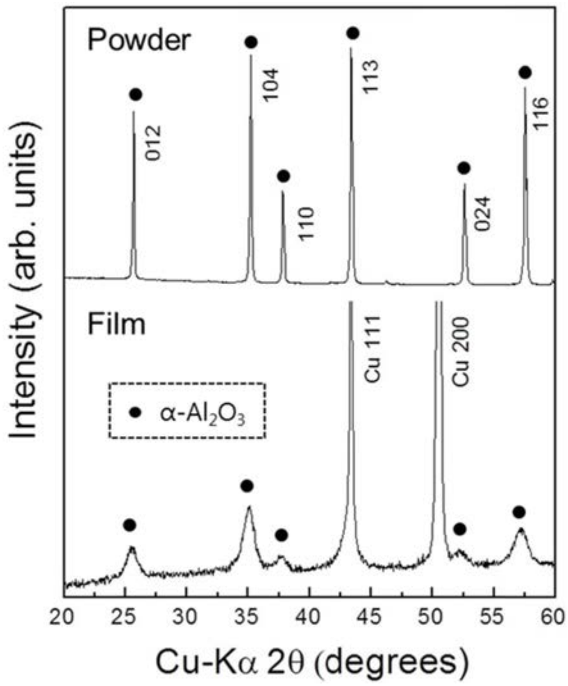

Fig. 3. XRD peak patterns of Al_2O_3 powders and Al_2O_3 thick films.

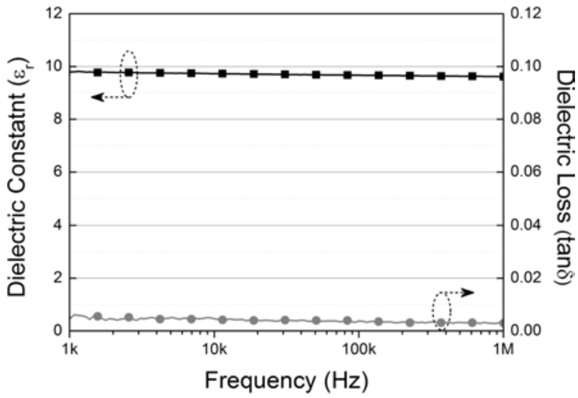

Fig. 4. Dielectric properties of the Al_2O_3 thick films at low-frequency range.

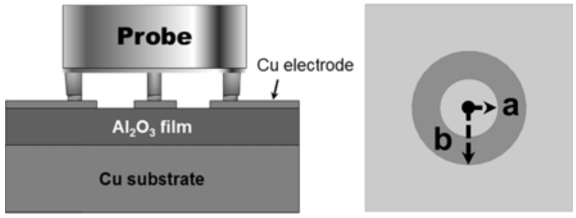

(a)

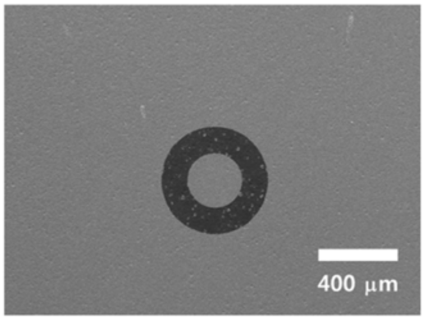

(b)

Fig. 5. (a) Schematic diagrams (cross-section and top view) of a circular-patch capacitor with GSG micro-probe. (b) SEM image of the fabricated circular-patch capacitor on the Al_2O_3 thick film.

using 0.5-μm Al_2O_3 powder. Fig. 3 shows the XRD patterns of both the powders and the thick films grown on the Cu substrates, which reveal a single Al_2O_3 phase without any second phases, despite being deposited at room temperature. However, peak broadening was observed in the XRD patterns due to residual stress and the small crystalline size. The crystalline size of the Al_2O_3 films was approximately 10 nm.

At first, low-frequency characterization of the Al_2O_3 thick film was carried out using an impedance analyzer with the typical metal-insulator-metal (MIM) structure. Fig. 4 shows the measurement results of the dielectric properties of the deposited films. The dielectric constant (ε_r) and the dielectric loss ($\tan\delta$) of the thick film deposited by the AD process were 9.6 and 0.004

at 100 kHz, respectively. Frequency dependence of both the ε_r and the tanδ was not observed due to the treatment of the starting powder and the post-processing of the deposited films.

Compared with low-frequency range, the characterization of dielectric properties at microwave frequency range is more complicated because parasitic components such as the metal electrodes and probe contact will influence the characterization as the frequency increases [21]. In order to avoid these parasitic components, several high-frequency characterization techniques of dielectric films with the specific test structure have been proposed [22-24]. The circular-patch capacitor (CPC) is one of the suitable geometries for the characterization of dielectric properties at microwave frequency range since it is easy to fabricate and it minimizes parasitic resistance and inductance [24]. The CPC geometry was used to measure the dielectric properties of Al_2O_3 film at microwave frequency range in this study as shown in Fig. 5(a). Moreover, in order to investigate the parasitic effects at microwave frequency, a simulation model for the CPC structure was designed using a 3-D EM simulator (HFSS), and these simulation results were compared with the measurement data.

For the measurement of reflection coefficients (S_{11}-parameters), the CPC structure with a thickness of 300 nm was patterned on the Al_2O_3 thick films through photo-lithography before e-beam evaporation as shown in Fig. 5(b). The S_{11}-parameters are easily converted to input impedance (Z_{in}) for the structure using the following equation:

$$Z_{in} = Z_0\left(\frac{1+S_{11}}{1-S_{11}}\right) \tag{1}$$

where Z_0 is the characteristic impedance (50-Ω). The simulated and measured S_{11}-parameters are plotted from 1 kHz to 6 GHz on a Smith chart as shown in Fig. 6. The simulated results show that the data were close to the outmost circle of the Smith chart, indicating that the CPC shows low-loss characteristics over the entire frequency range. Although it is seen that the simulation results are consistent with the experimental results, a discrepancy between the simulation and measurement results was still observed, likely stemming from the parasitic effect of the CPC structure.

The CPC consists of an inner capacitor and an outer capacitor surrounding it, with these capacitors formed on the bottom metal. As the frequency increases, so does the influence of the parasitic components, such as the parasitic resistance due to the top/bottom metal and the parasitic capacitance caused by the outer ground, which affects the input impedance of the CPC. To obtain the pure dielectric properties in the CPC structure at microwave frequency, the parasites should be removed. In order to minimize the parasitic effect of the outer capacitor, the impedance of the CPC with a large inner diameter ($Z_{in,2}$) was subtracted from that of the CPC with a small inner diameter ($Z_{in,1}$) as shown in following equation [24]:

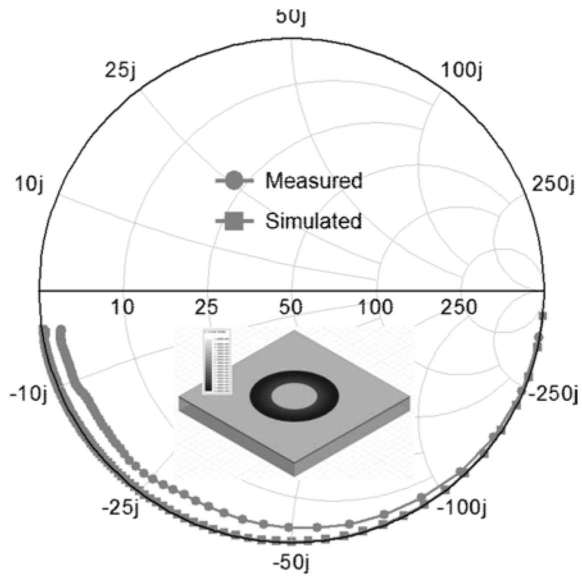

Fig. 6. Measured and simulated S_{11}-parameters of the circular-patch capacitor plotted on a Smith chart.

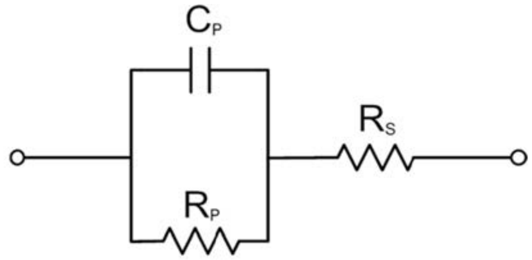

(a)

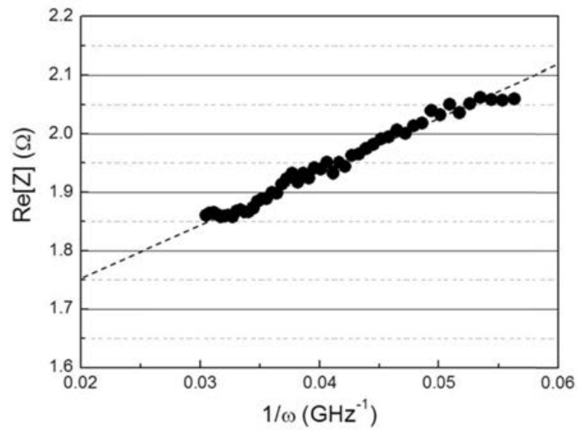

(b)

Fig. 7. (a) Equivalent-circuit model for the circular-patch capacitor. (b) Fitting process of the parasitic resistance R_s.

$$Z_{in,1}-Z_{in,2}=-\frac{1}{\omega\varepsilon_0\varepsilon_r}\frac{d}{}\left(\frac{1}{a_1^2}-\frac{1}{a_2^2}\right) \quad (2)$$

where a_1 and a_2 are the diameters of the inner capacitor of the CPC, and ε_0 the permittivity of free space (8.854×10^{-12} F/m), ε_r is the complex dielectric constant of the Al_2O_3 film, d is the thickness of the thick film, and ω is the angular frequency. Thus, two types of CPC ($a_1 = 140$ μm, $a_2 = 260$ μm, $b = 275$ μm) on the Al_2O_3 thick films were prepared in this study. In addition, the contact resistance between the electrodes and the micro-probe along with the parasitic resistance due to the top/bottom metal was also considered. An equivalent circuit model was introduced to remove the parasitic effects from these resistances as shown in Fig. 7(a). The series resistance (R_s) represents the parasitic components from the top/bottom metal and the probe contact, and the parallel resistance (R_p) and capacitance (C_p) represent the pure components from the dielectric films. The loss tangent of the dielectric film can be expressed as follows:

$$\tan\delta_d=\frac{Re(Z_{in})-R_s}{In(Z_{in})} \quad (3)$$

$$Re(Z_{in})=Im(Zin)\times\tan\delta_d+R_s=-\frac{1}{\omega C_p}\times\tan\delta_d+R_s \quad (4)$$

When the frequency is infinite in Eq. (3), the R_s is the same as the Re (Z_{in}). Thus, the R_s can be obtained by a least square fitting [25] of the measured data as shown in Fig. 7(b). The tan δ_d can be calculated from Eq. (4). The fitting range was chosen from 1 GHz to 6 GHz considering the instrumental sensitivity. Fig. 8 shows the measured tanδ of the Al_2O_3 film before and after correction of the R_s. The frequency dependence of the tanδ was remarkably reduced after correction of the contact resistance. It was observed that the ε_r of the Al_2O_3 thick films was 9.7 at 1 GHz, which was very similar to the result at low frequency range, and the ε_r slightly decreased with an increase in frequency whereas there was no such frequency dependence at frequencies below 1 MHz. The tand of the Al_2O_3 thick films was 0.03 at 1 GHz and less than 0.05 up to 5 GHz.

These results are very important in terms of high-frequency device design such as a planar device based on the dielectric substrate because the device size and performance are highly dependent on dielectric properties of the substrate. A 50-ohm microstrip line, which is most commonly used planar device for RF and microwave applications, was designed using these measurement results at 5-GHz, and the size and performance of the microstrip line were compared with that of using low-frequency measurement results. As shown in Table 2, it was confirmed that the device size and insertion loss under 50-ohm matching condition increase when using high-frequency results.

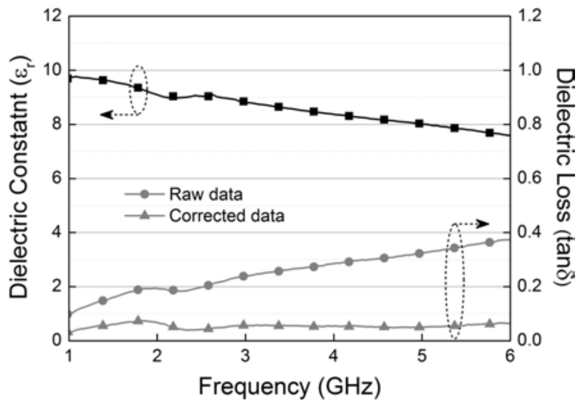

Fig. 8. Dielectric properties of the Al_2O_3 thick films at high-frequency range.

Table 2. Comparison of simulation results of a 50-ohm microstrip line (μ-line) at 5-GHz using low- and high-frequency measurement results.

Simulation frequency	5 GHz	5 GHz
Thickness of substrate	0.5 mm	0.5 mm
Permittivity of substrate	9.6 (measured at 100 kHz)	8 (measured at 5 GHz)
Loss tangent of substrate	0.004 (measured at 100 kHz)	0.05 (measured at 5 GHz)
Line width of μ-line	500 μm	520 μm
Return loss of μ-line	> 40 dB	> 40 dB
Insertion loss of μ-line	0.09 dB/cm	0.54 dB/cm

Conclusions

Dense Al_2O_3 thick films were fabricated through the AD process before a heat treatment and ball milling of the starting powder in order to improve the ultimate dielectric properties of the thick films. The dielectric properties of the Al_2O_3 thick films were investigated at both low- and high-frequency ranges. The dielectric properties were effectively measured using a circular-patch capacitor (CPC) and an equivalent-circuit model in the microwave frequency range. 3-D electromagnetic simulation results revealed the parasitic effect of the CPC structure. Compared to the results of the low-frequency range, the corrected dielectric constant of the Al_2O_3 thick films was slightly decreased with the increased of frequency, from 9.7 at 1 GHz. The corrected dielectric losses of the Al_2O_3 thick films were 0.03 at 1 GHz and less than 0.05 up to 5 GHz.

Acknowledgements

This work was supported by the Nuclear Power Core Technology Development Program of the Korea Institute of Energy Technology Evaluation and Planning (KETEP), granted financial resource from the Ministry of Trade, Industry & Energy, Republic of Korea. (No. 20131520000190).

References

1. T.S. Rappaport, S. Sun, R. Mayzus, H. Zhao, Y. Azar, K. Wang, G.N. Wong, J.K. Schulz, M. Samimi, and F. Gutierrez, IEEE Access 1(2013)335-349.
2. W. Hong, K.H. Baek, Y. Lee, Y. Kim, and S.T. Ko, IEEE Commun. Mag. 52[9] (2014) 63-69.
3. R.R. Tummala, IEEE Trans. Adv. Packag. 27[2] (2004) 241-249.
4. K.W. Lee, A. Noriki, K. Kiyoyama, T. Fukushima, T. Tanaka, and M. Koyanagi, IEEE Trans. Electron Devices 58[3] (2011) 748-757.
5. M. Lahti and V. Lantto, J. Eur. Ceram. Soc. 21[1] (2001) 1997-2000.
6. A.A. Shapiro, L. Martha, and H.P. Lee, Microelectronics J. 33[5-6] (2002) 443-447.
7. J. Akedo, J. Therm. Spray. Tech. 17[2] (2008) 181-198.
8. J. Akedo, J. Am. Ceram. Soc. 89[6] (2006) 1834-1839.
9. D.W. Lee, H.J. Kim, Y.N. Kim, M.S. Jeon, and S.M. Nam, Surf. Coat. Technol. 209 (2012) 160-168.
10. D.W Lee, M.C. Shin, Y.N. Kim, and J.M. Oh, Ceram. Int. 43 (2017) 1044-1051.
11. H.J. Kim, Y.H. Kim, Y.J. Yoon, J.H. Kim, and S.M. Nam, J. Korean Phys. Soc. 57(2010) 1086-1091.
12. D.W. Lee and S.M. Nam, J. Ceram. Process. Res. 11[1] (2010) 100-106.
13. D.W. Lee, H.J. Kim, Y.H. Kim, Y.H. Yun, and S.M. Nam, J. American Ceram. Soc. 94[9] (2011) 3131-3138.
14. Y. H. Kim, J. W. Lee, H. J. Kim, Y. H. Yun, and S. M. Nam, Ceram. Int., 38[1](2012)S201-S204.
15. O.Y. Kwon, H.J. Na, H.J. Kim, D.W. Lee, and S.M. Nam, Nanoscale Res. Lett. 7[261] (2012) 1-8.
16. H.J. Kim and S.M. Nam, J. Ceram. Process. Res. 10[6] (2009) 817-822.
17. D.W. Lee, H.J. Kim, and S.M. Nam, J. Korean Phys. Soc. 57 (2010) 1115-1121.
18. S.M. Nam, M. Momotani, N. Mori, H. Kakemoto, S. Wada, J. Akedo, and T. Tsurumi, Integr. Ferroelectr. 66 (2004) 301-310.
19. M. Momotani, N. Mori, S. M. Nam, H. Kakemoto, S. Wada, T. Tsurumi, and J. Akedo, Key Eng. Mater. 301 (2006) 117-120.
20. J.W. Lee and J.H. Koh, J. Nanosci. Nanotechno. 15 (2015) 2300-4.
21. D.C. Dube, J. Baborowski, P. Muralt, and N. Sett, Appl. Phys. Lett. 74[23] (1999) 3546-3548.
22. K. Ikura, Y Umeda, and Y Ishii, Jpn. J. Appl. Phys. 34 (1995) L1211-L1213.
23. P. Bao, T.J. Jackson, X. Wang, and M.J. Lancaster, J. Phys. D. 41[6] (2008) 1-21.
24. Z. Ma, A.J. Becker, P. Polakos, H. Huggins, J. Pastalan, H. Wu, K. Watts, Y.H. Wong, and P. Mankiewich, IEEE Trans. Electron Devices 45 (1998) 1811.
25. W. Chang, C. Gilmore, W. Kim, J. Pond, S. Kirchoefer, S. Qadri, D. Chrisey, and J. Horwitz, J. Appl. Phys. 87[6] (2000) 3044-3049.